

Supplementary Information:

Ship Hull Form Design Intelligence with Generative Technology
and Evolutionary Algorithms

1. MATERIALS

1.1 SHIPS2PIX ENCODER

In the Ships2pix encoder, we first discretize the 3D hull model along the draft direction to extract the waterlines. These discrete waterlines are then further sampled along the ship's length to obtain surface point cloud data. Once the point cloud is acquired, the coordinates are normalized in the longitudinal (L), beam (B), and draft (T) directions. Subsequently, the normalized X and Y coordinates of the point cloud are extracted as pixel values, resulting in a two-channel image representation. The detailed procedure is depicted in Fig. S1.

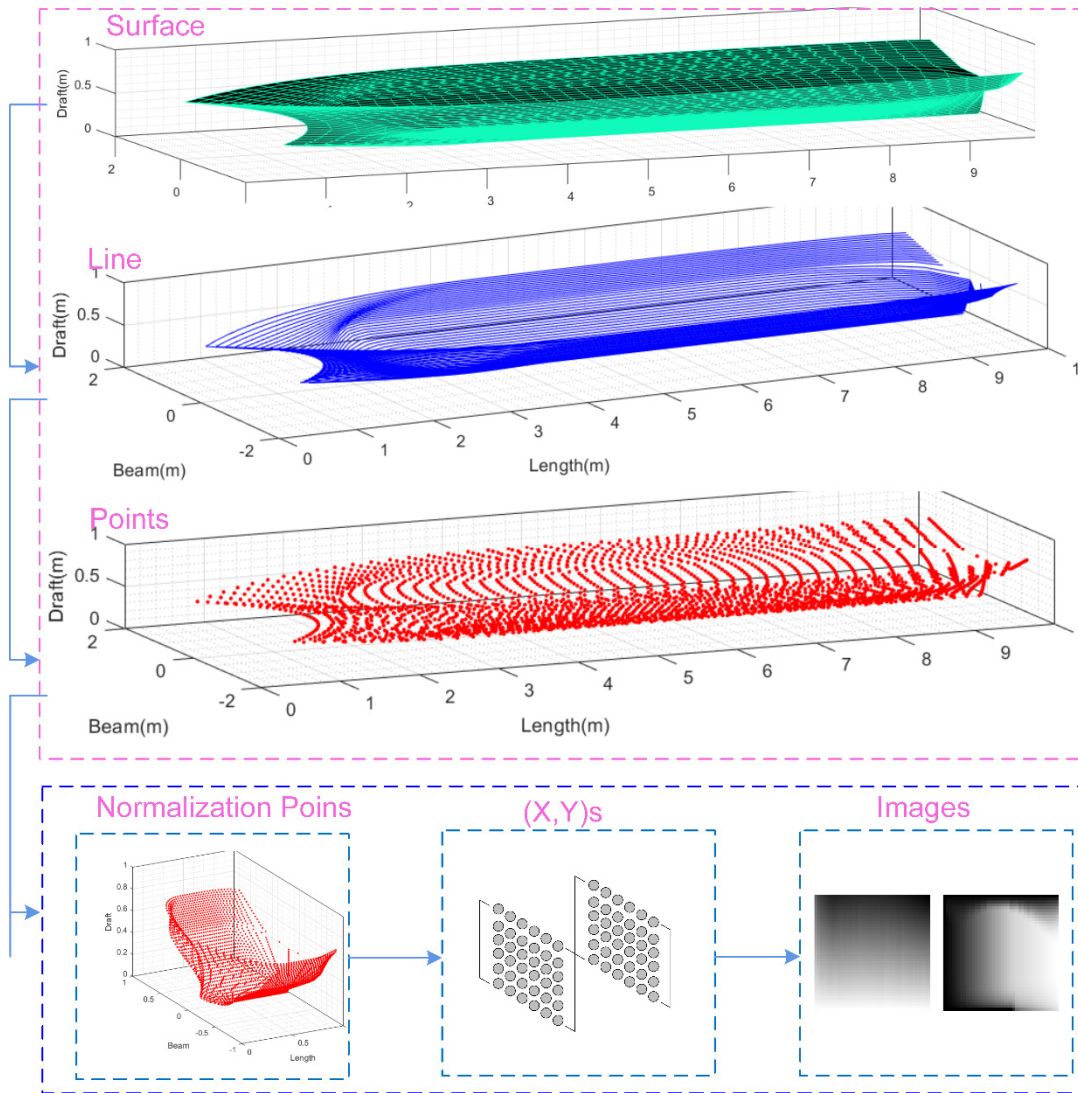


Fig. S1: The detailed procedure of Ship2pix encoder

1.2 THE ARCHITECTURE OF GENERATOR

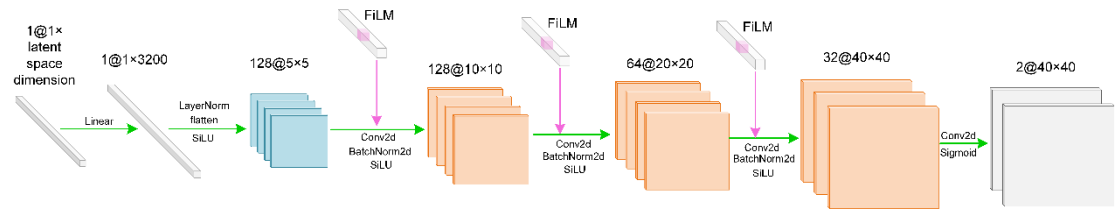


Fig. S2: The detailed architecture of generator.

1.3 THE ARCHITECTURE OF DISCRIMINATOR

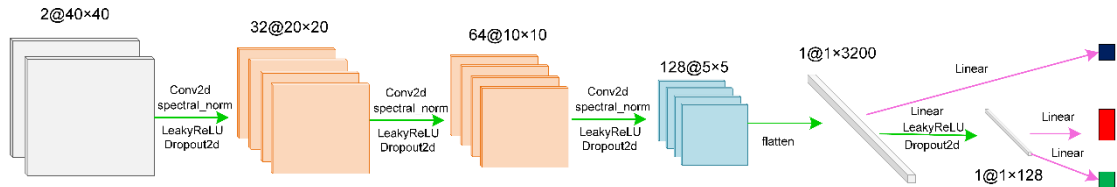


Fig. S3: The detailed architecture of discriminator.

1.4 5-DIMENSIONAL LATENT SPACE RESULT

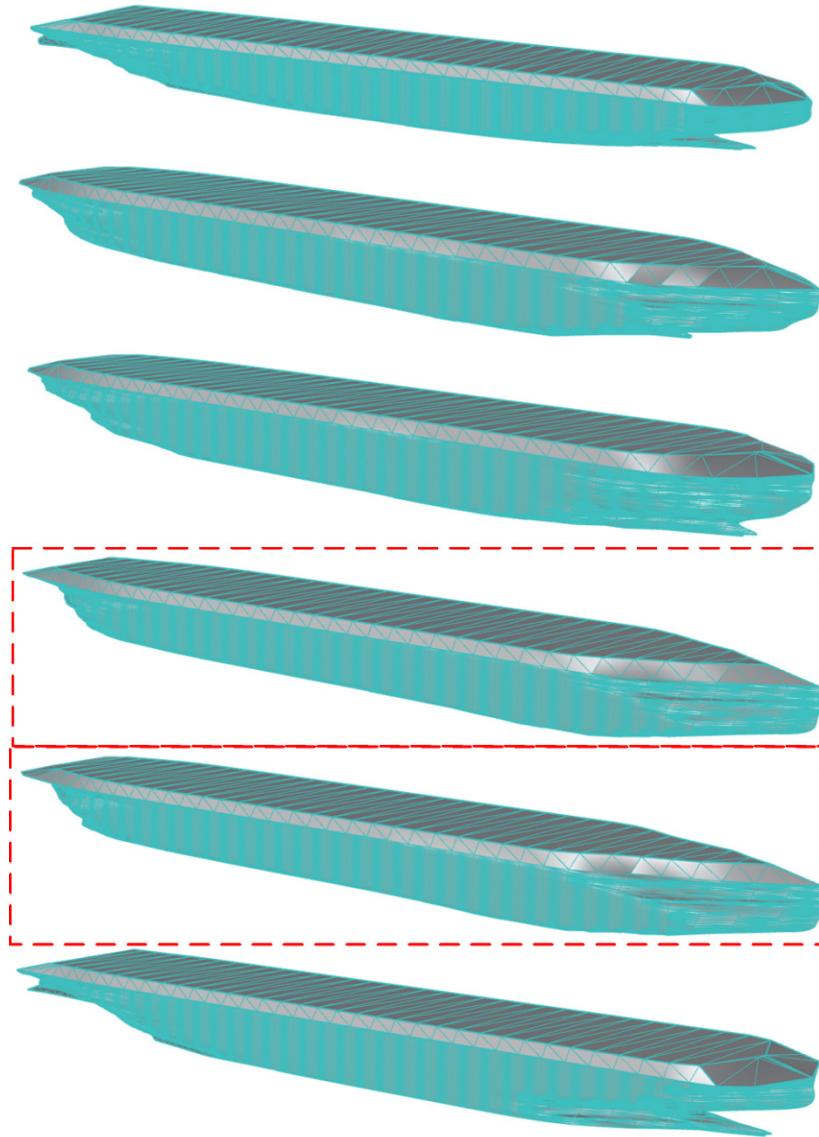


Fig. S4: Set the bow shape as the bulbous bow to generate the Hull form scheme (latent space=5D).

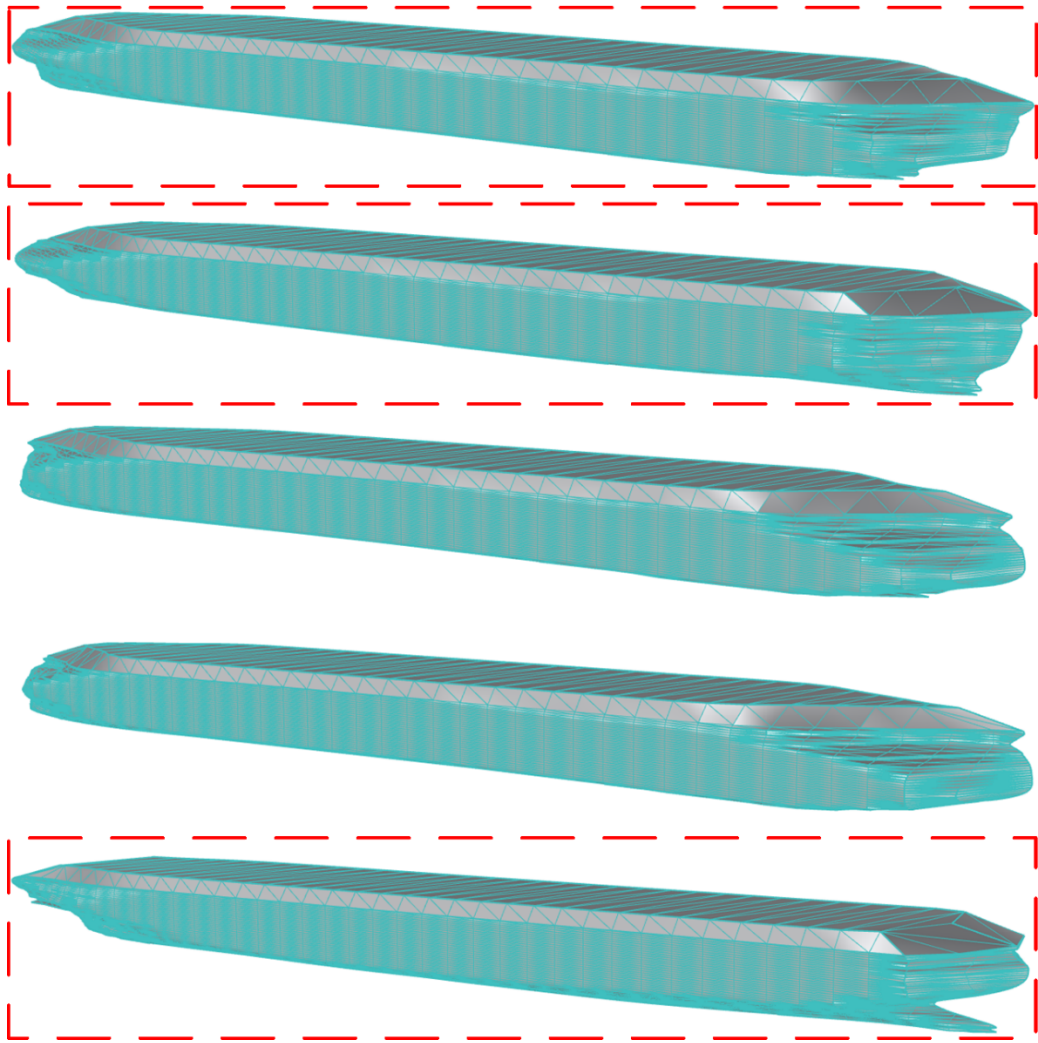
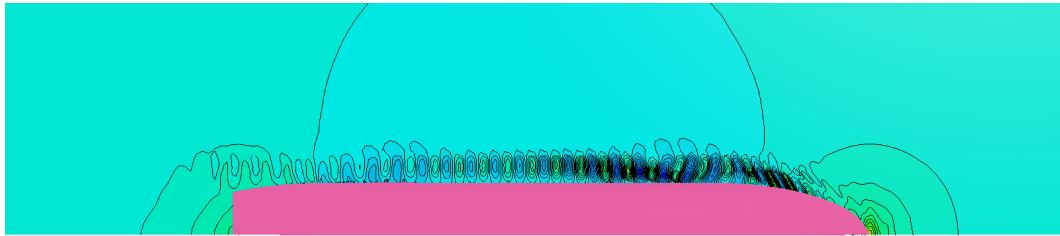


Fig. S5: Set the bow shape as the notbulbous bow to generate the Hull form scheme (latent space=5D).

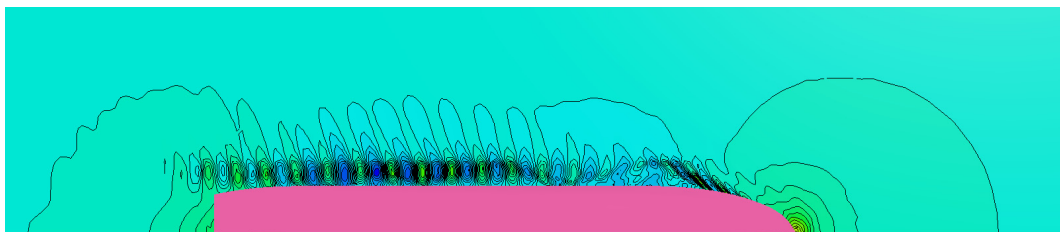
2. RANS RESULT

The free surface result of *Designer Scheme*:



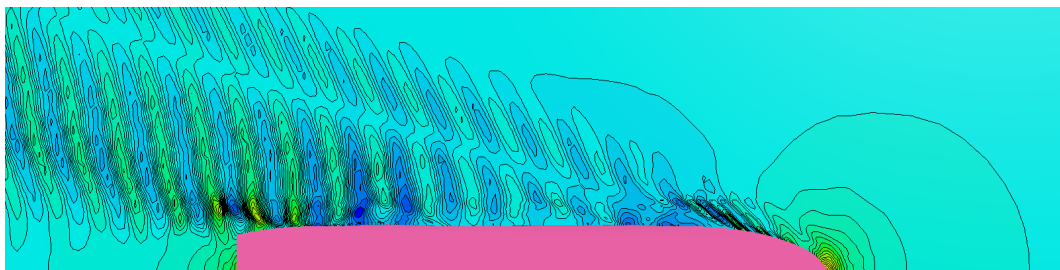
Position[Z] (m)
-0.00493 0.00367 0.0123

$V_s = 5kn$



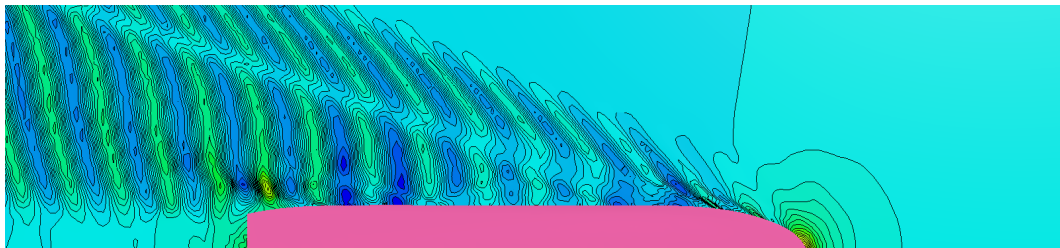
Position[Z] (m)
-0.00619 0.00404 0.0143

$V_s = 6kn$



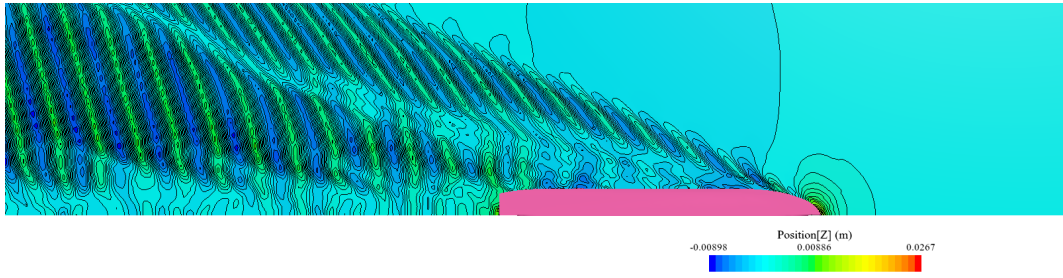
Position[Z] (m)
-0.00533 0.00464 0.0146

$V_s = 7kn$

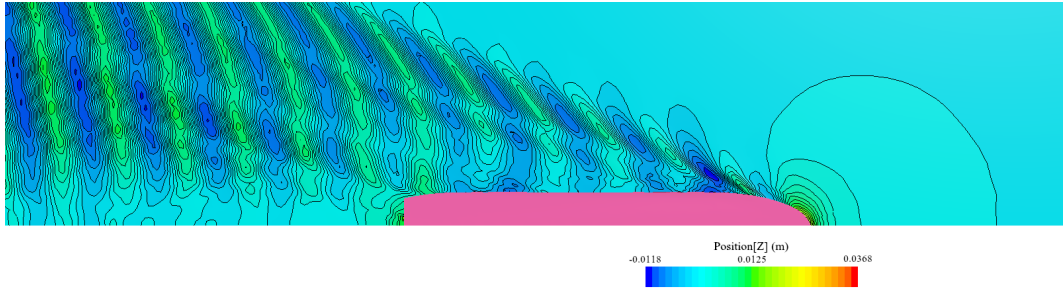


Position[Z] (m)
-0.00692 0.00689 0.0207

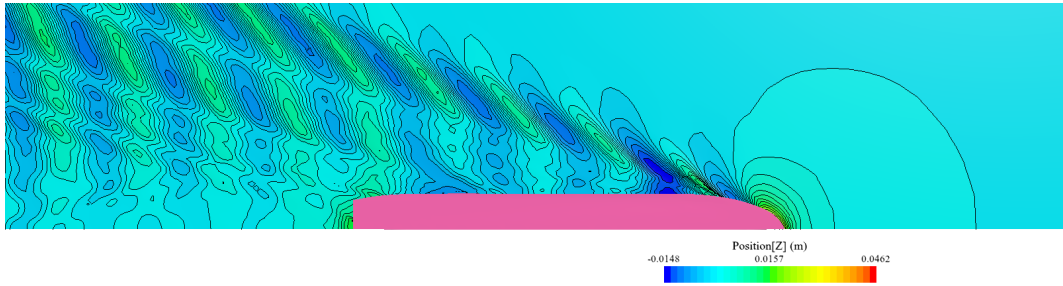
$V_s = 8kn$



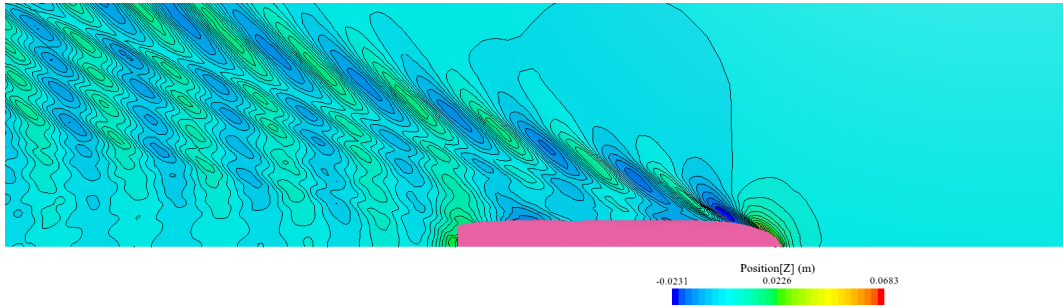
$V_s = 9kn$



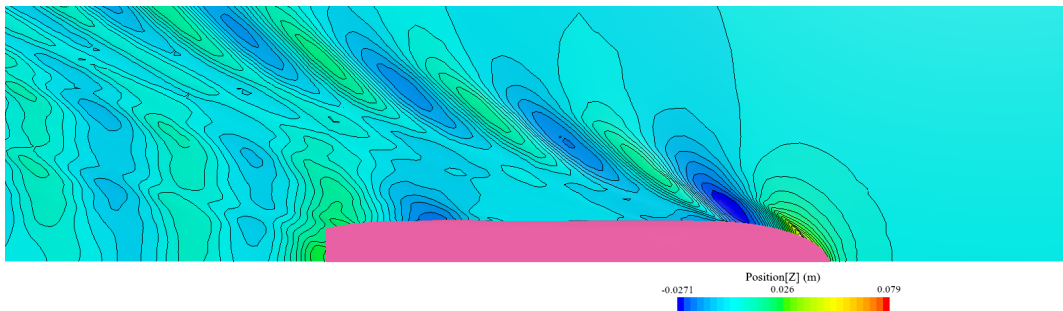
$V_s = 10kn$



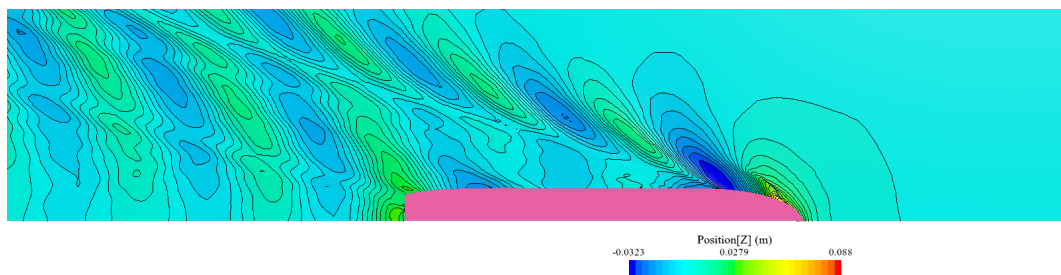
$V_s = 11kn$



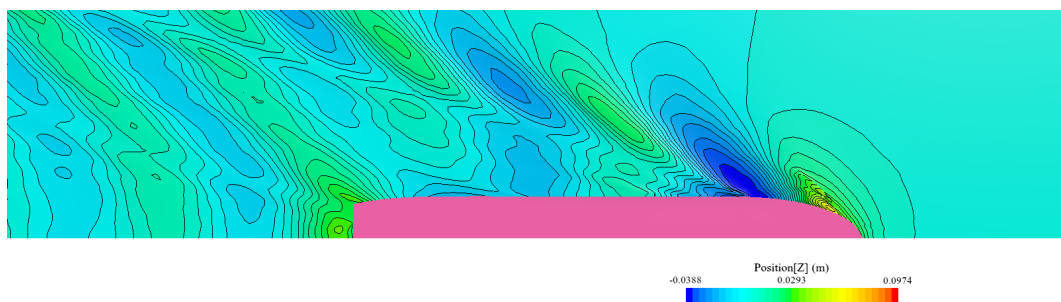
$V_s = 13kn$



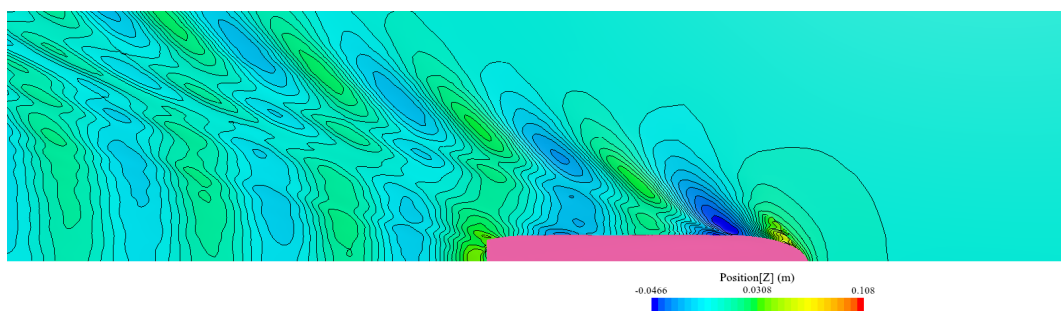
$V_s = 14kn$



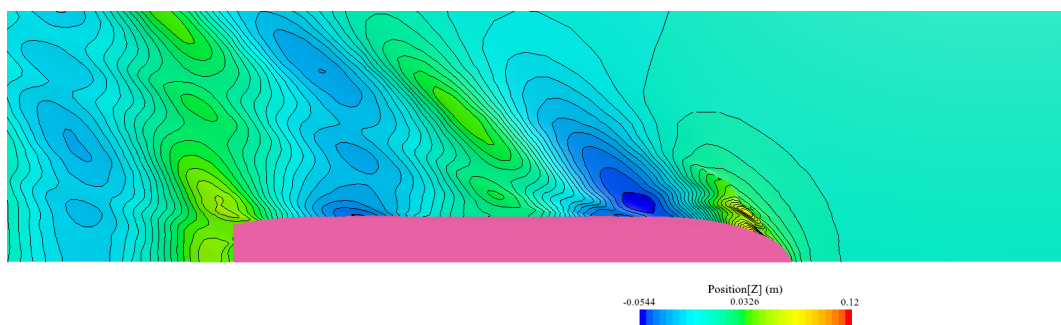
$V_s=15kn$



$V_s=16kn$

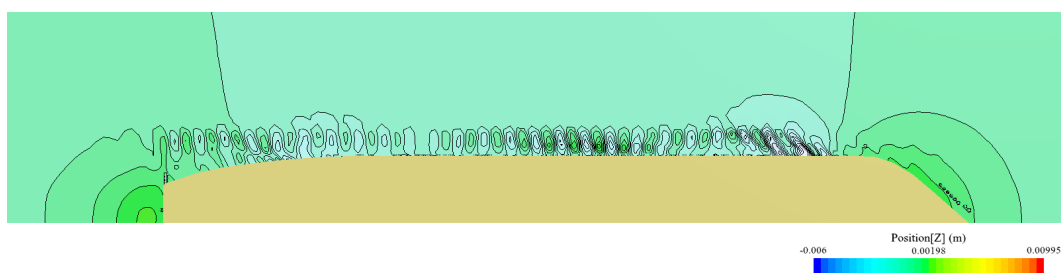


$V_s=17kn$

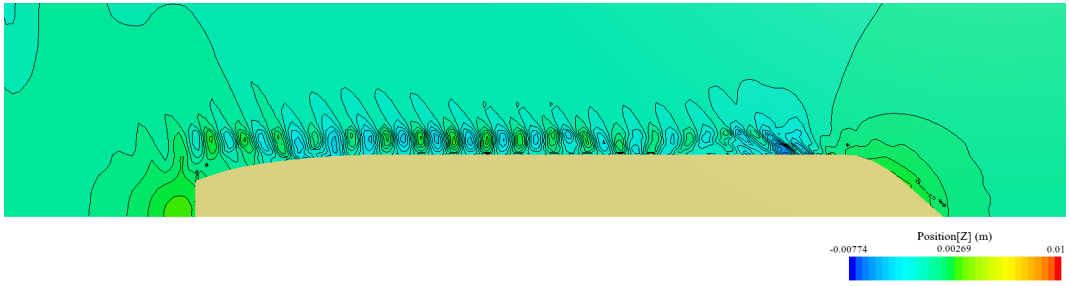


$V_s=18kn$

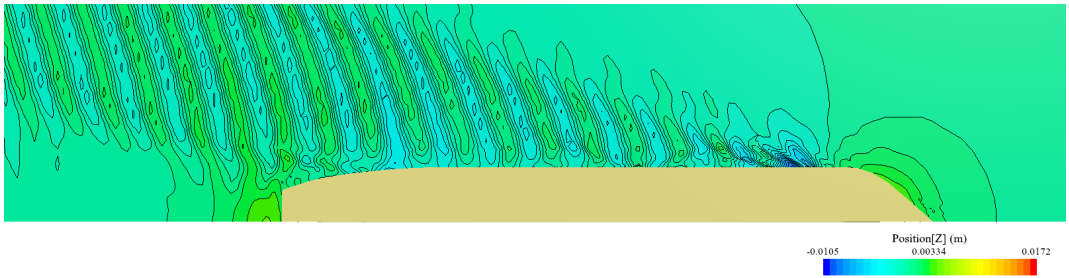
The free surface result of *ShipDMaster-DNO.1*:



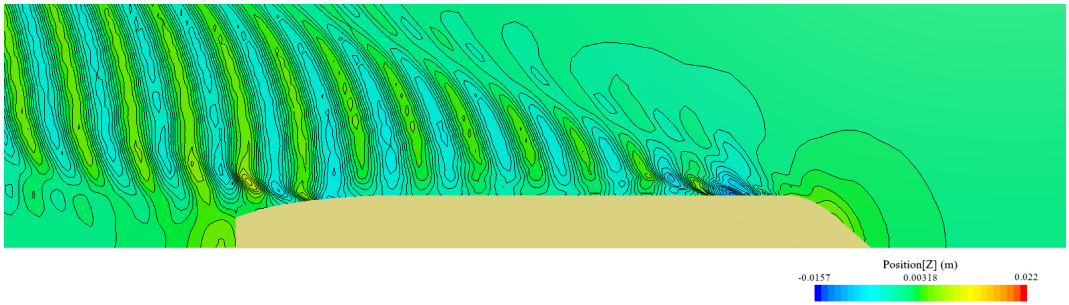
$V_s=5kn$



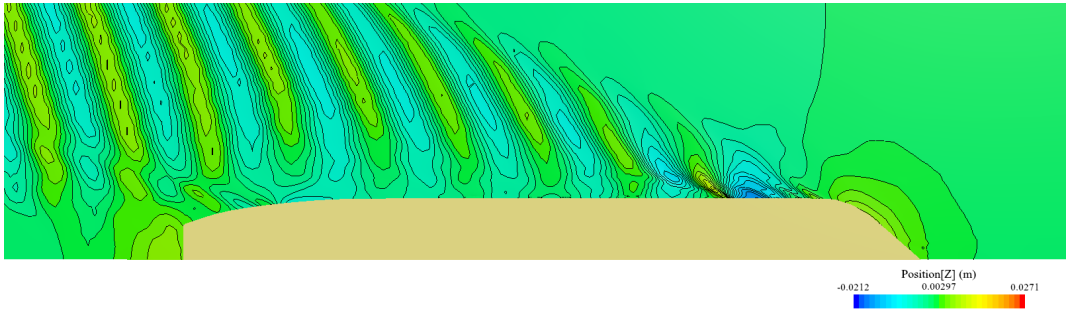
$V_s = 6kn$



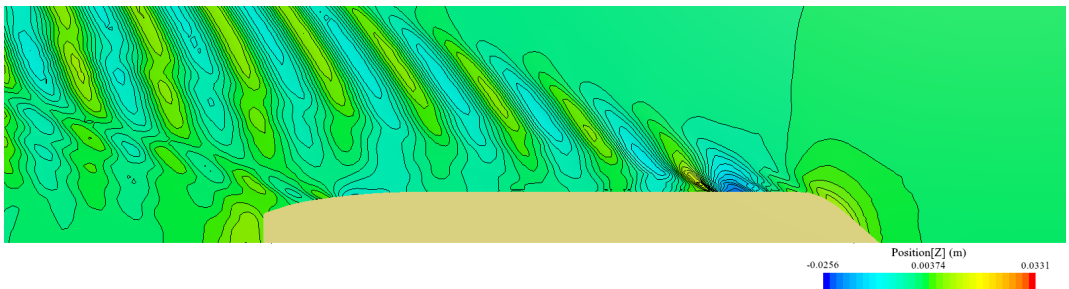
$V_s = 7kn$



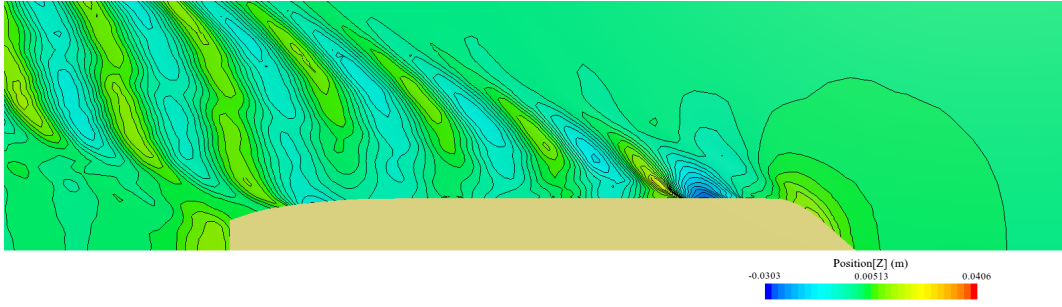
$V_s = 8kn$



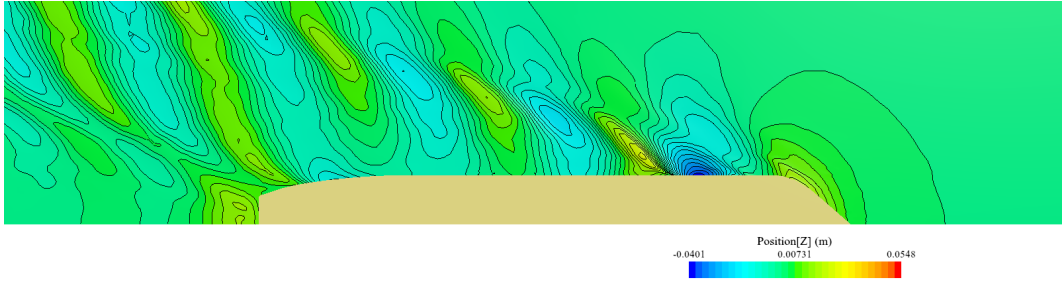
$V_s = 9kn$



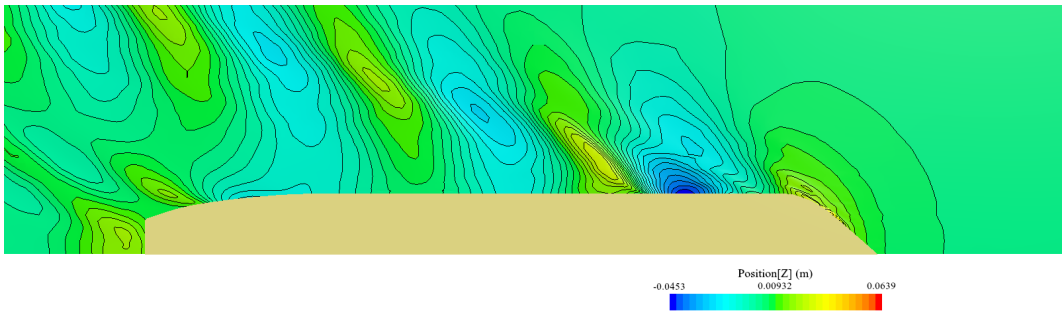
$V_s = 10kn$



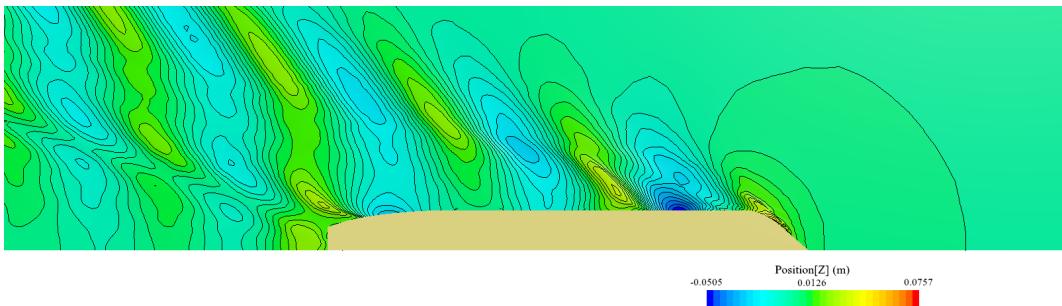
$V_s = 11kn$



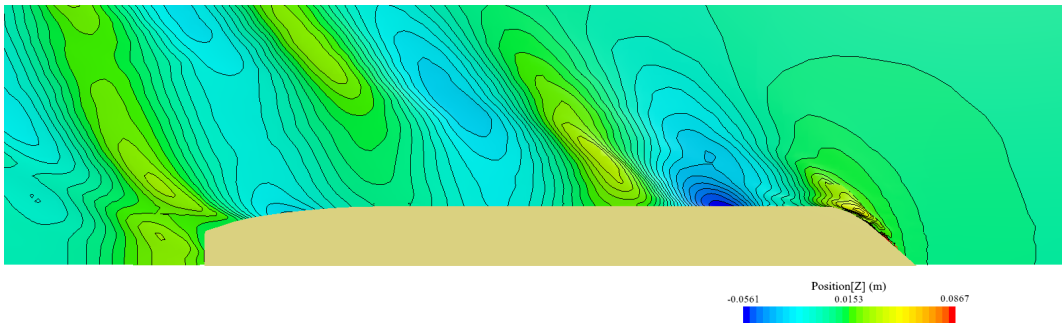
$V_s = 13kn$



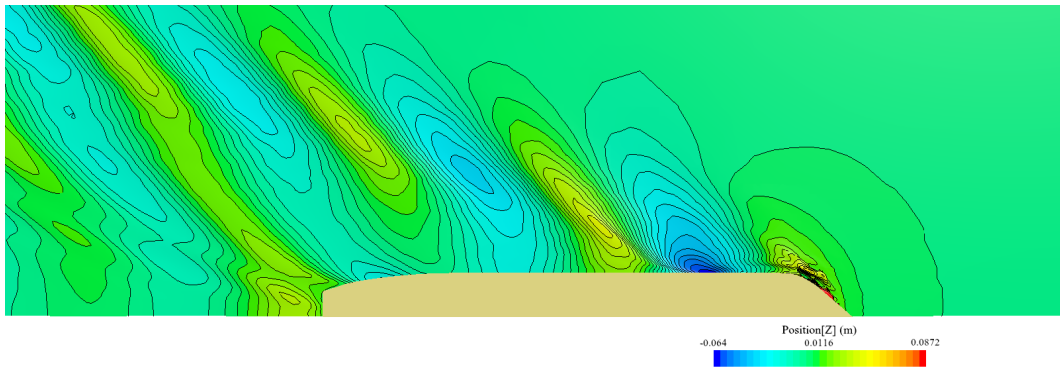
$V_s = 14kn$



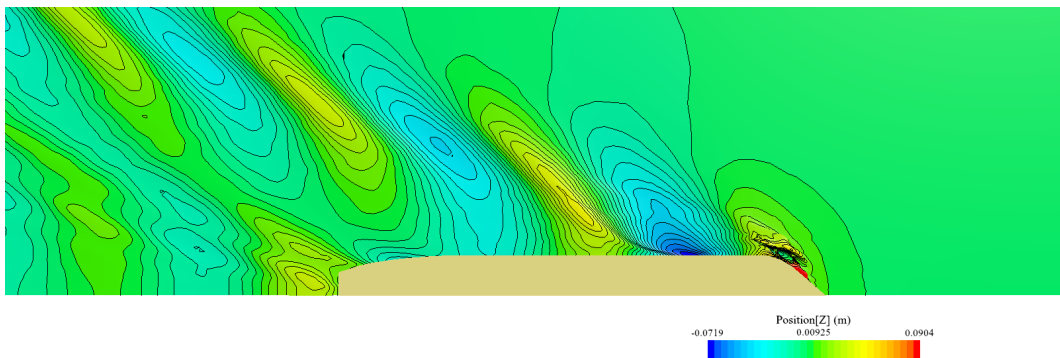
$V_s = 15kn$



$V_s = 16kn$

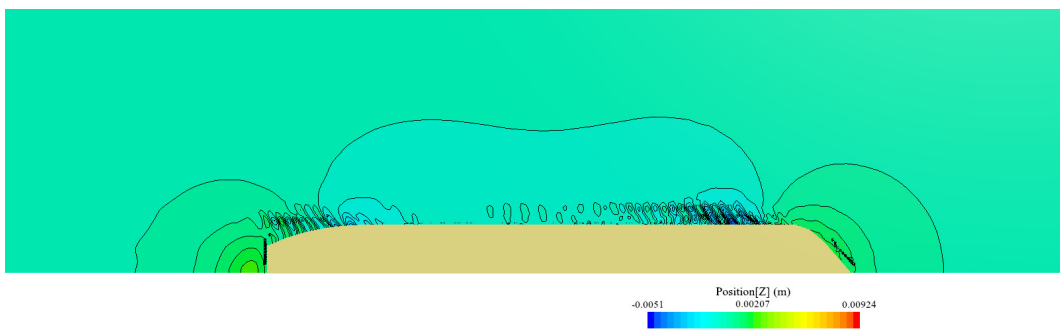


$V_s = 17kn$

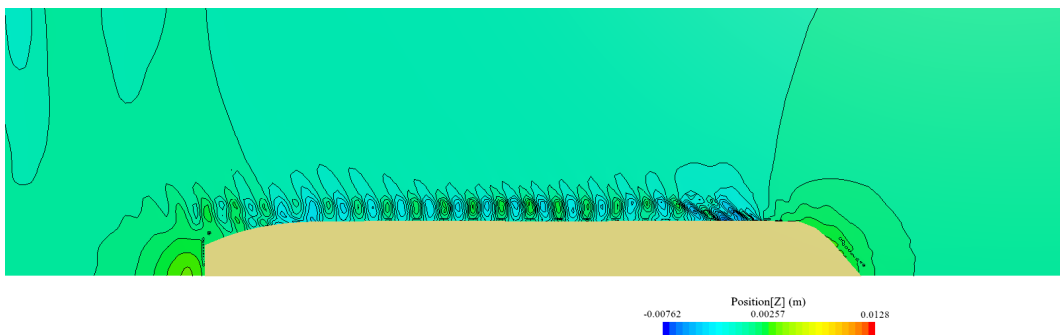


$V_s = 18kn$

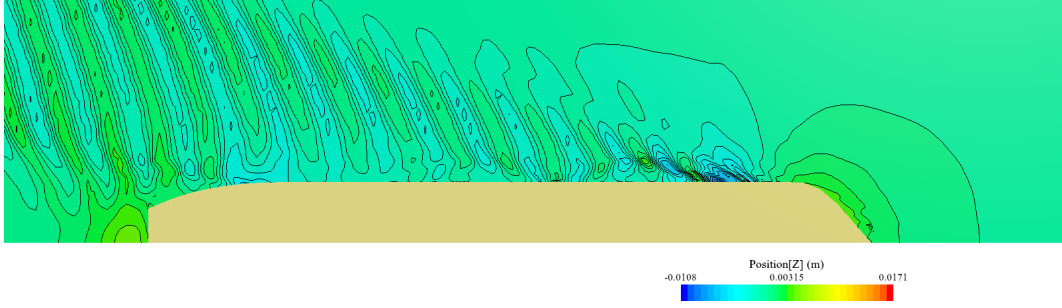
The free surface result of *ShipDMaster-DNO.2*:



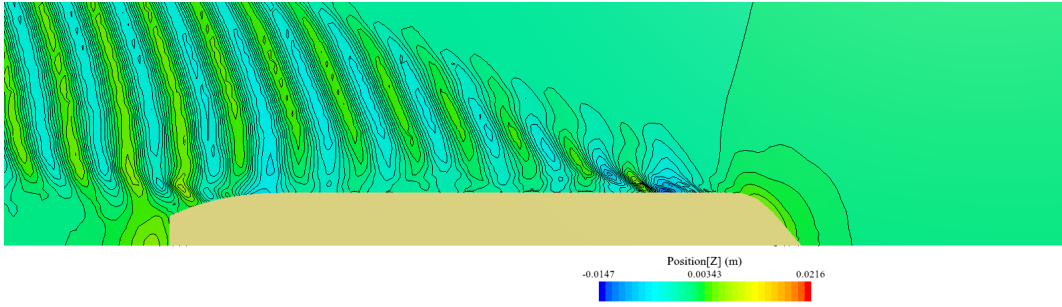
$V_s = 5kn$



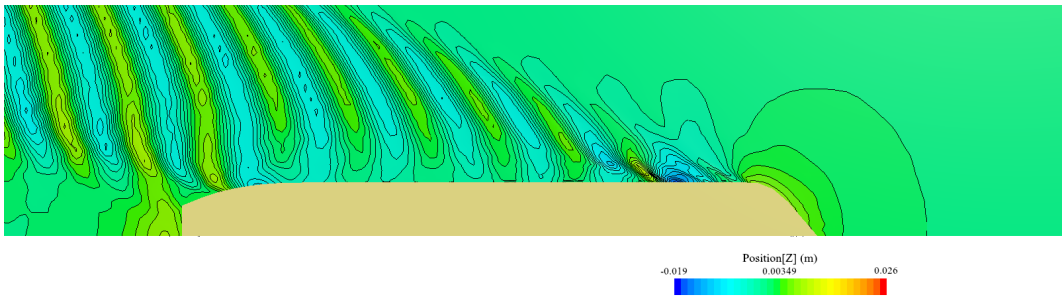
$V_s = 6kn$



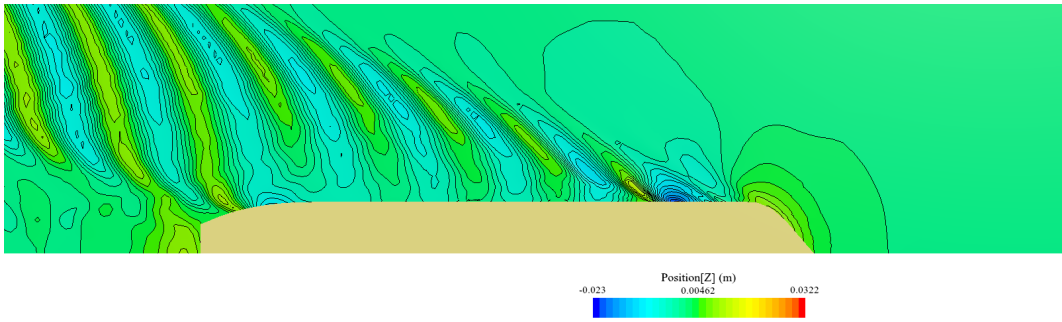
$$V_s = 7kn$$



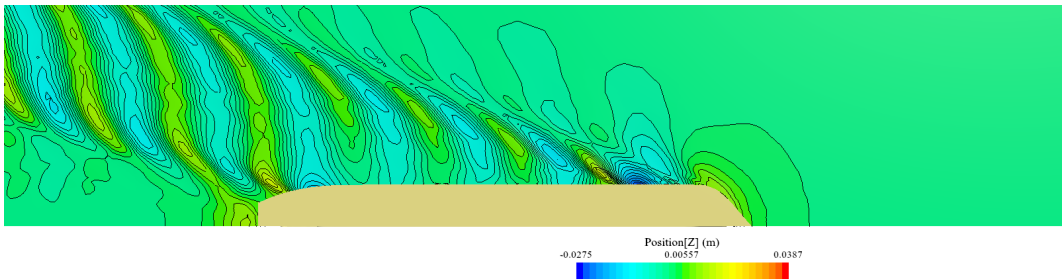
$$V_s = 8kn$$



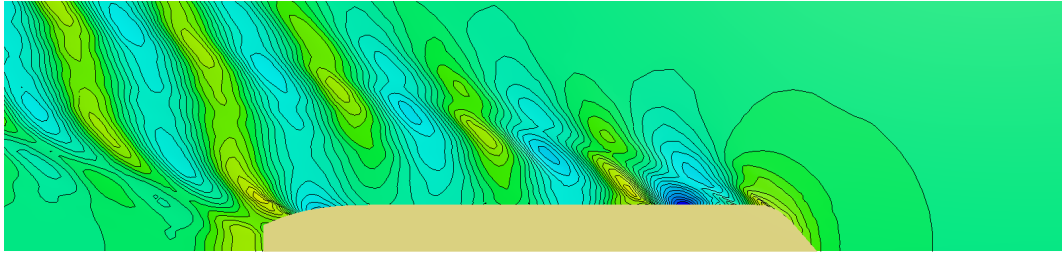
$$V_s = 9kn$$



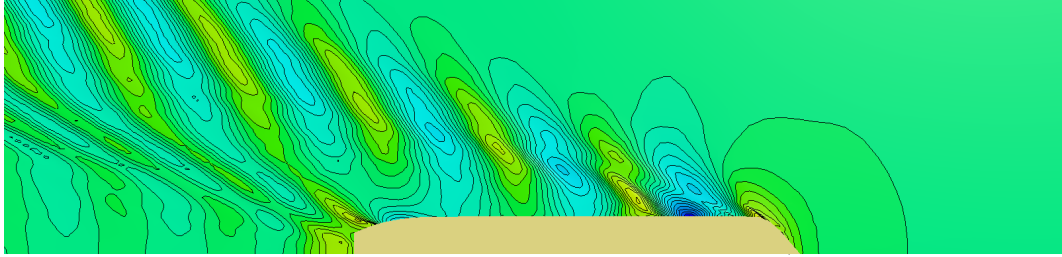
$$V_s = 10kn$$



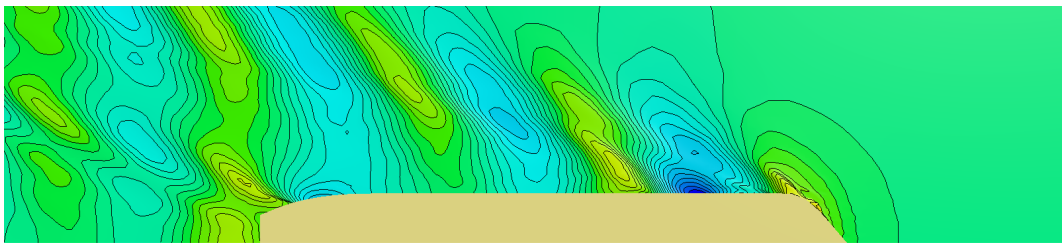
$$V_s = 11kn$$



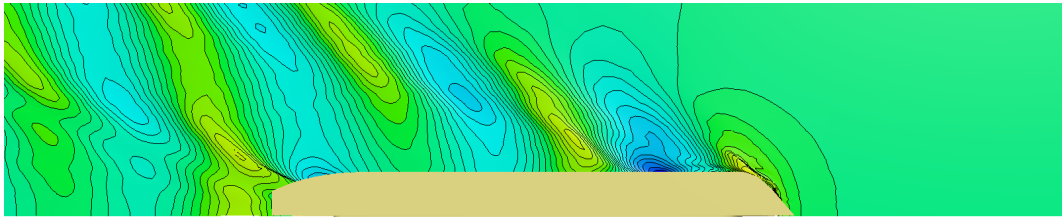
$V_s=13kn$



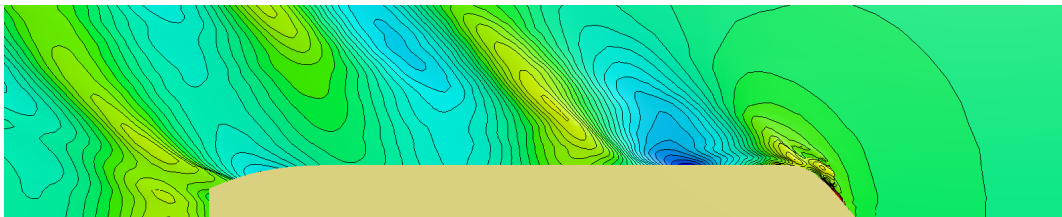
$V_s=14kn$



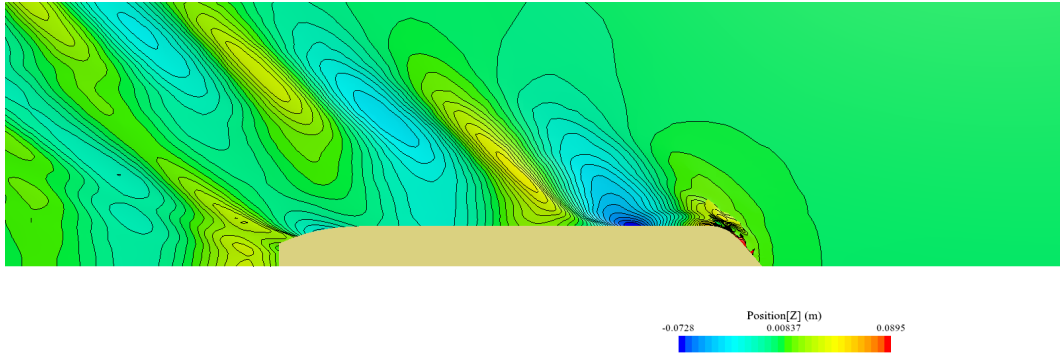
$V_s=15kn$



$V_s=16kn$

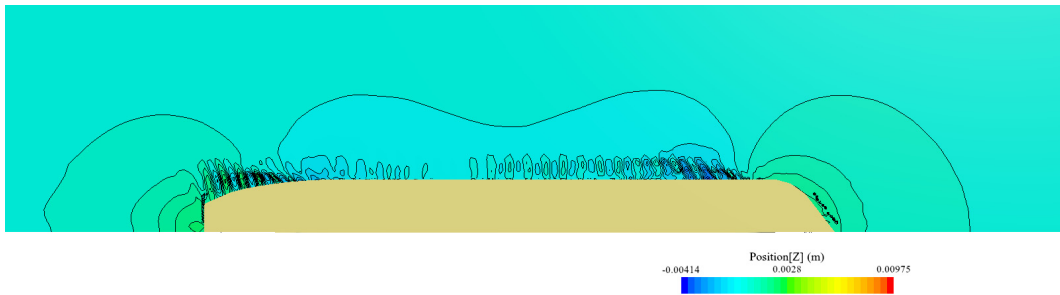


$V_s=17kn$

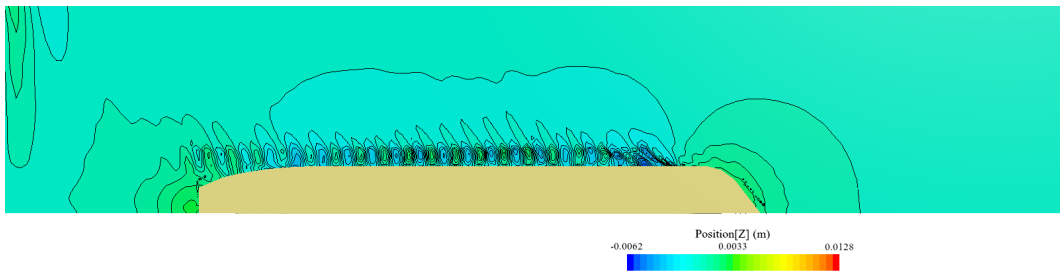


$$V_s = 18 \text{ kn}$$

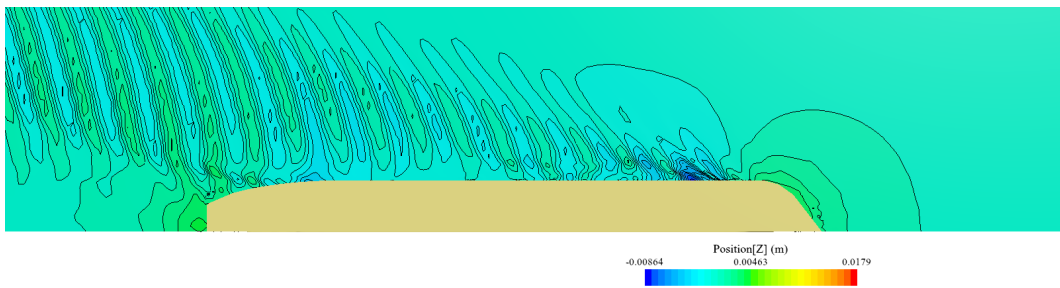
The free surface result of *ShipDMaster-DNO.3*:



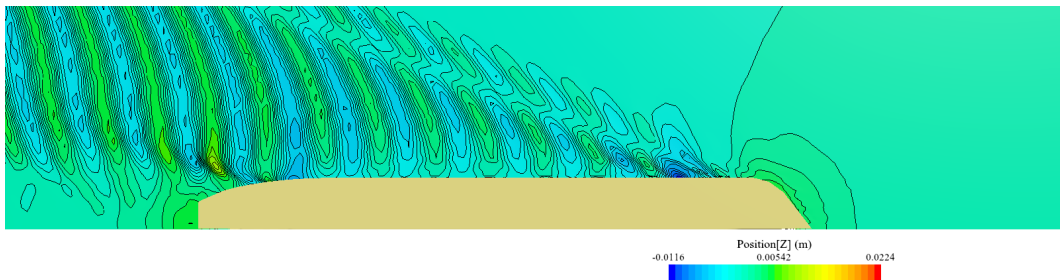
$$V_s = 5 \text{ kn}$$



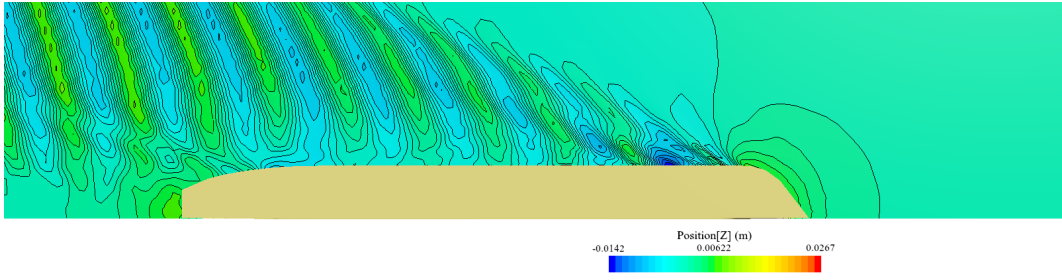
$$V_s = 6 \text{ kn}$$



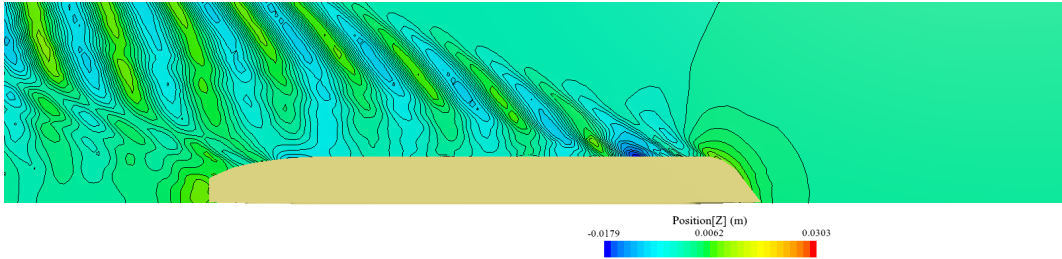
$$V_s = 7 \text{ kn}$$



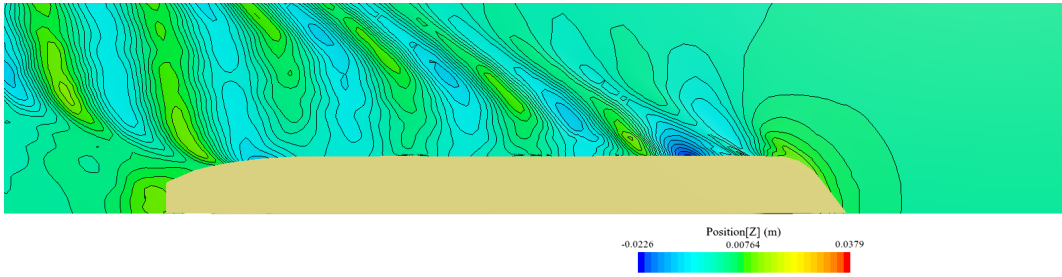
$$V_s = 8 \text{ kn}$$



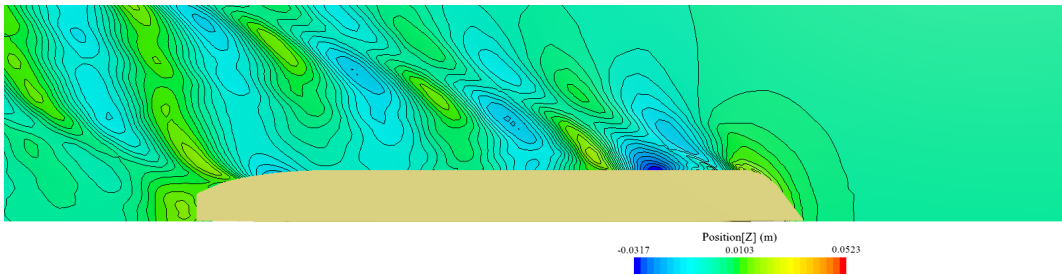
$V_s = 9kn$



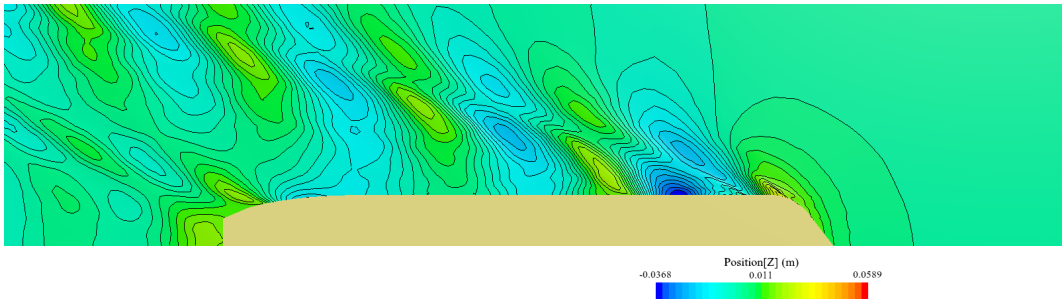
$V_s = 10kn$



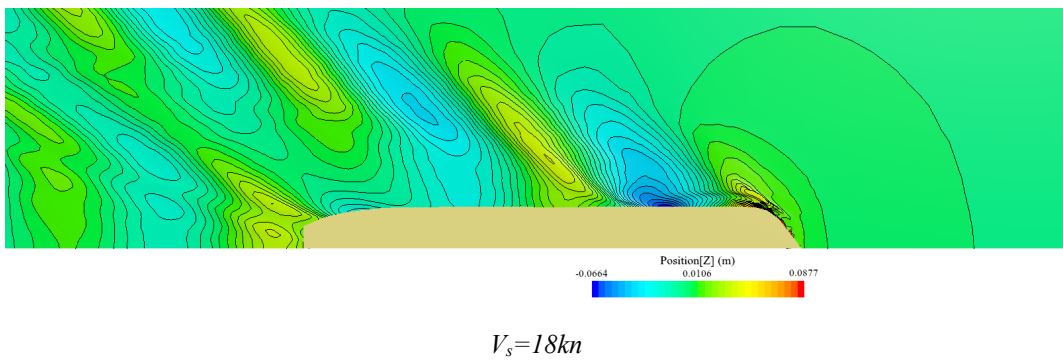
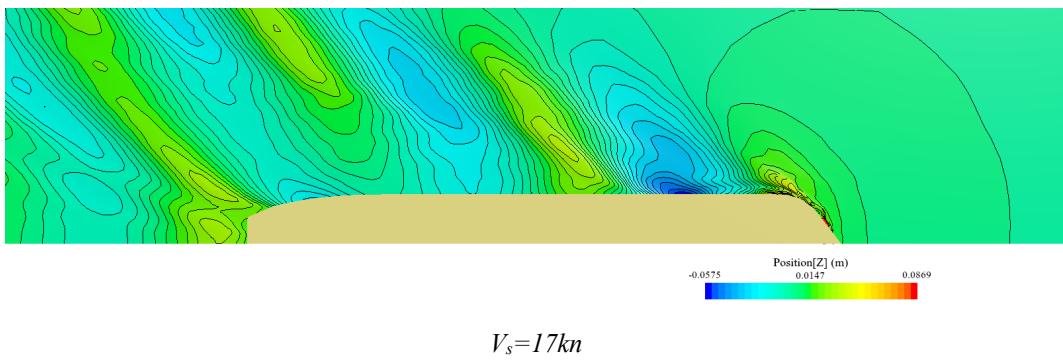
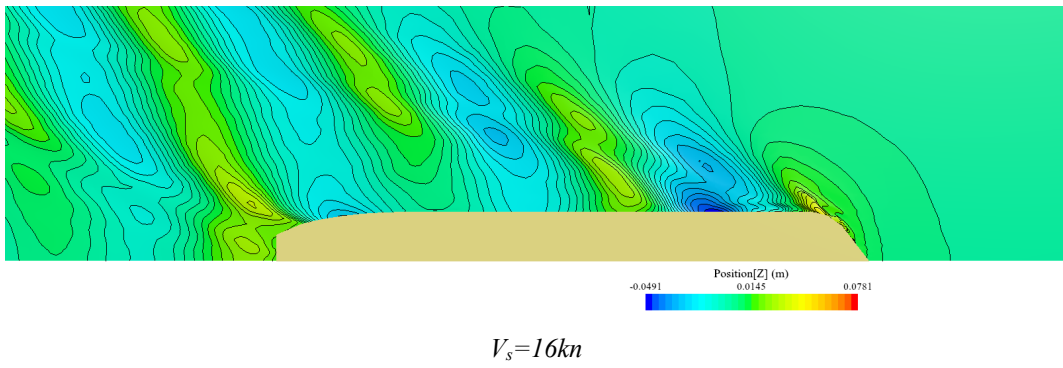
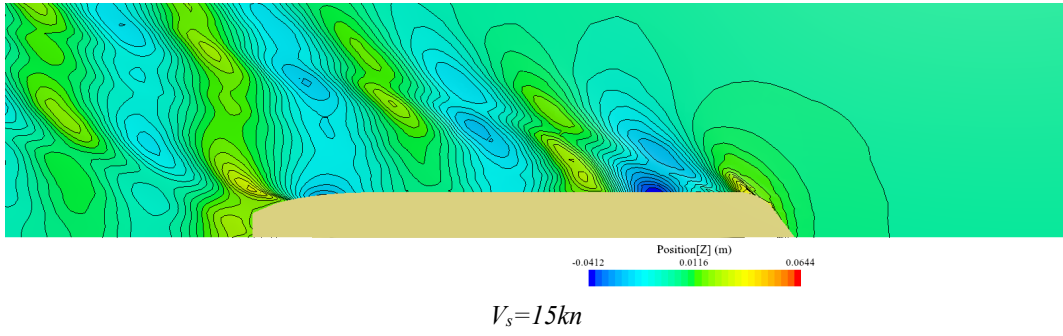
$V_s = 11kn$



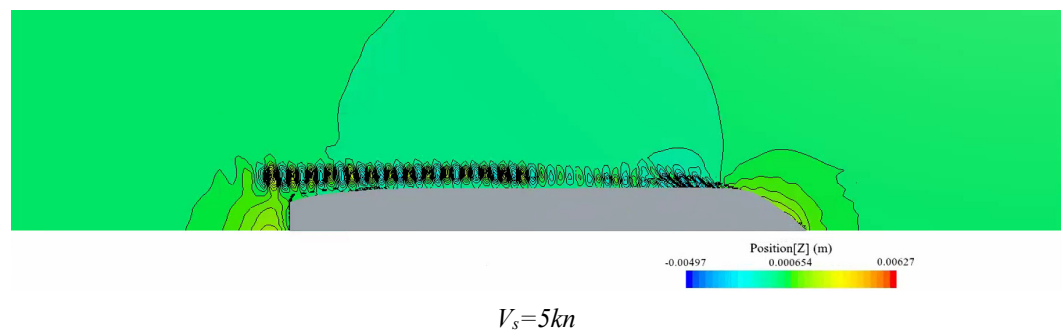
$V_s = 13kn$

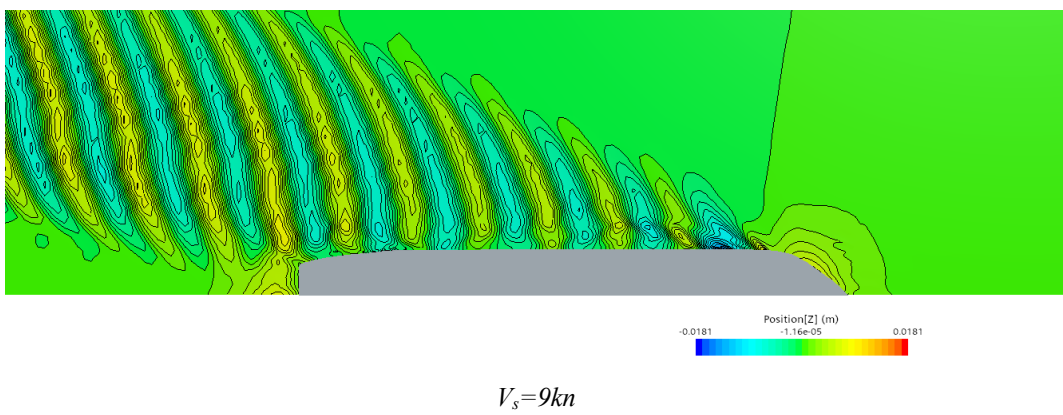
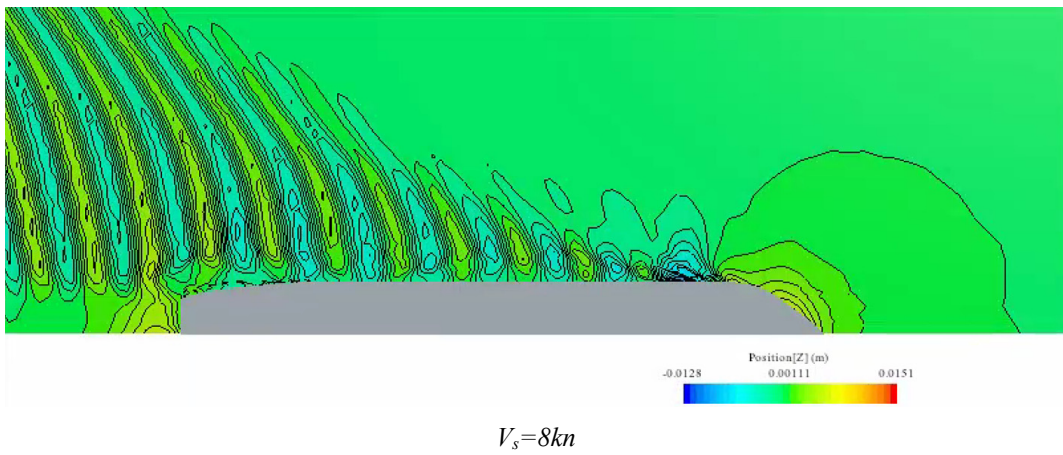
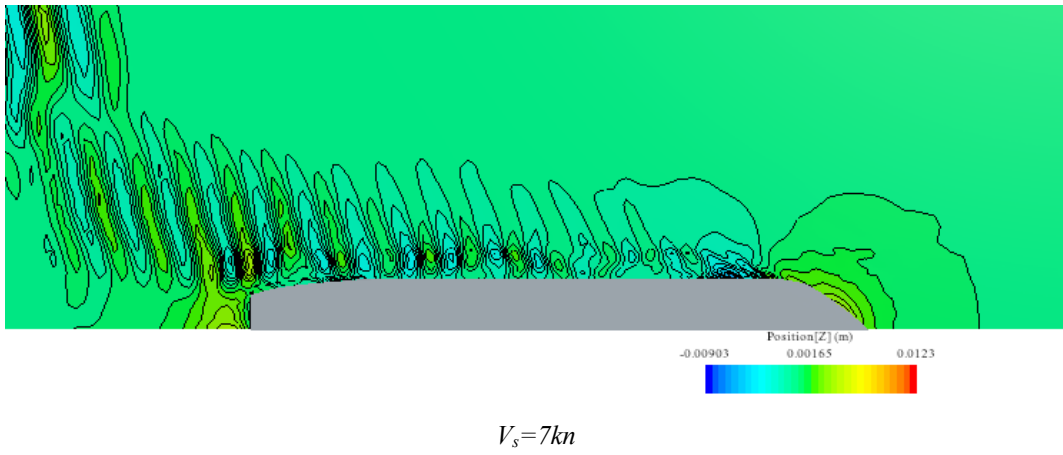
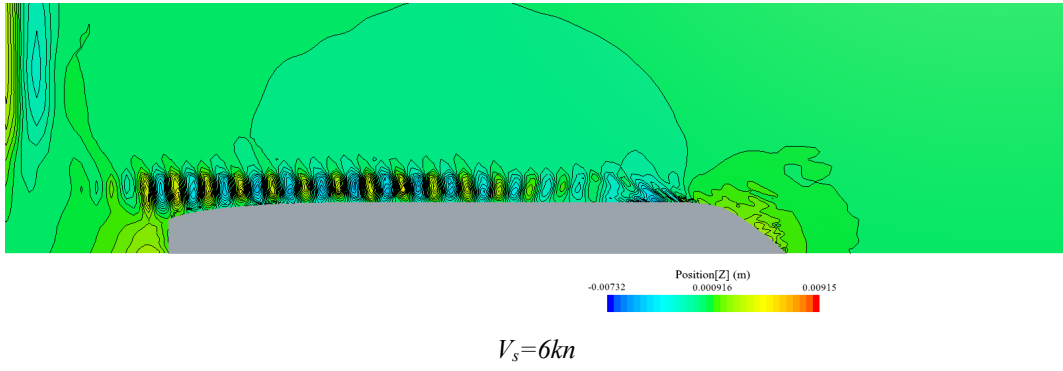


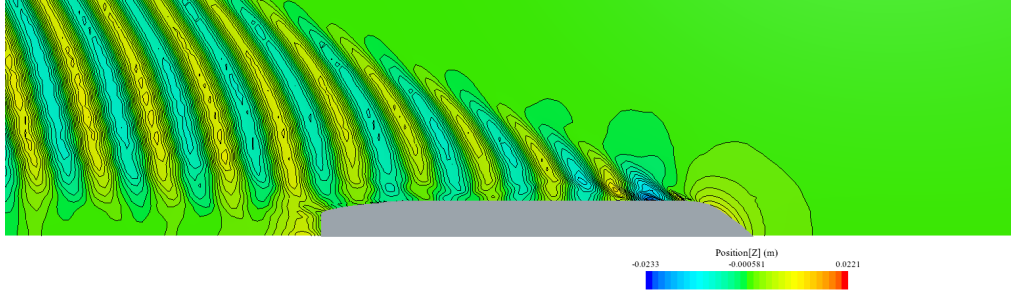
$V_s = 14kn$



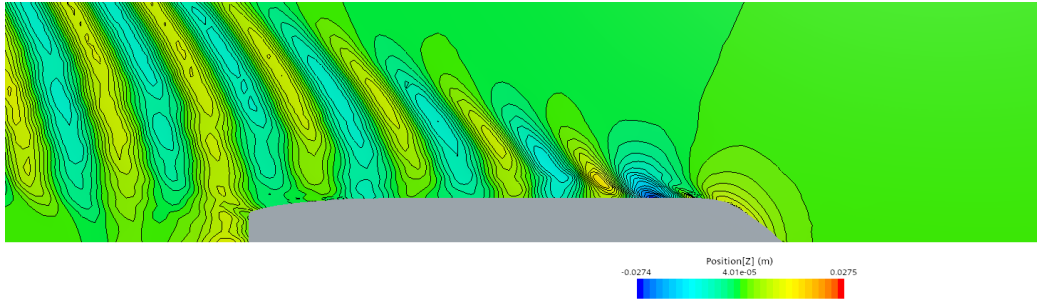
The free surface result of *ShipDMaster-Opt*:



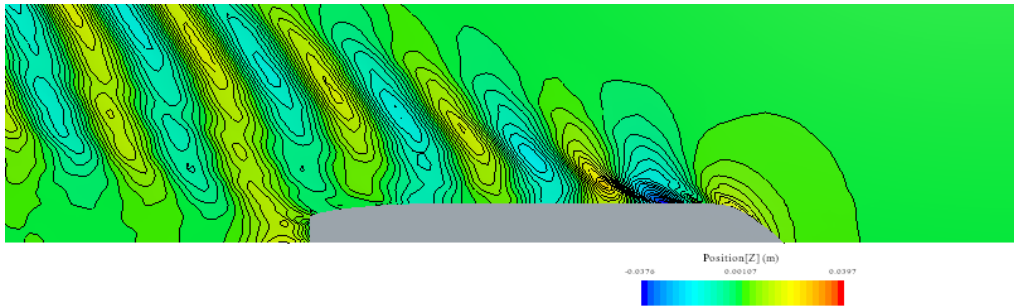




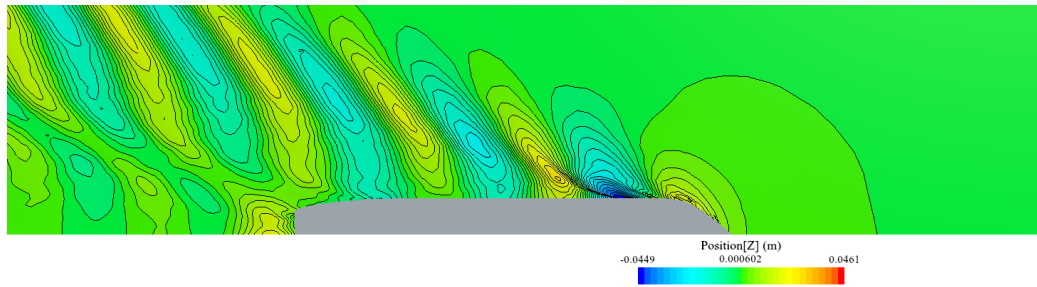
$V_s = 10kn$



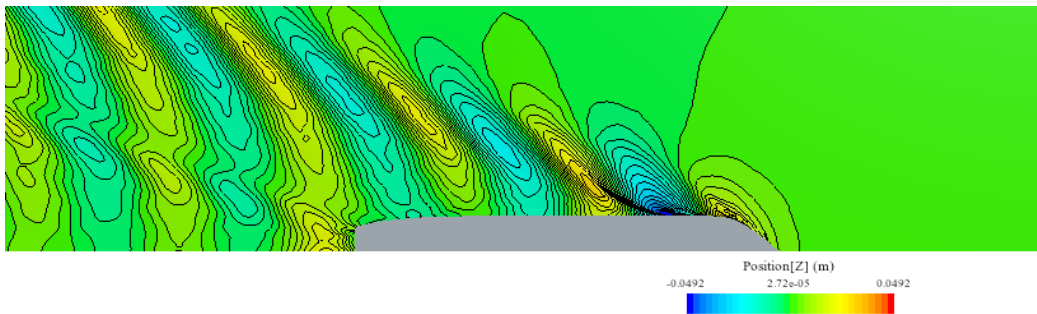
$V_s = 11kn$



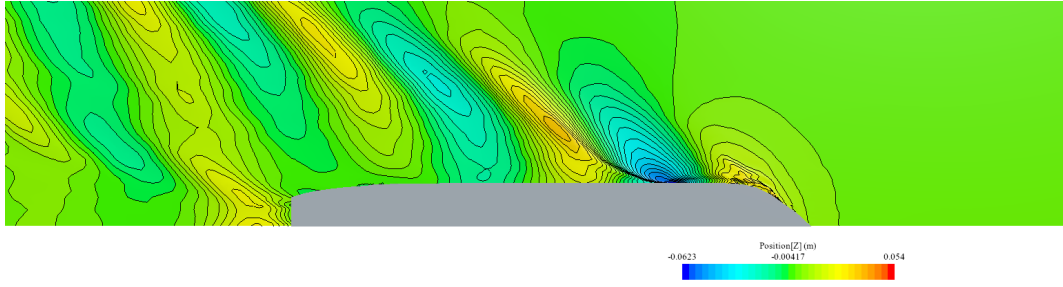
$V_s = 13kn$



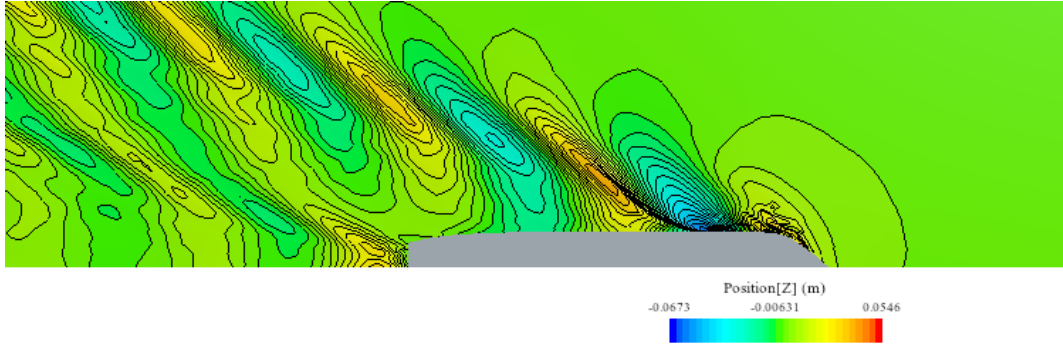
$V_s = 14kn$



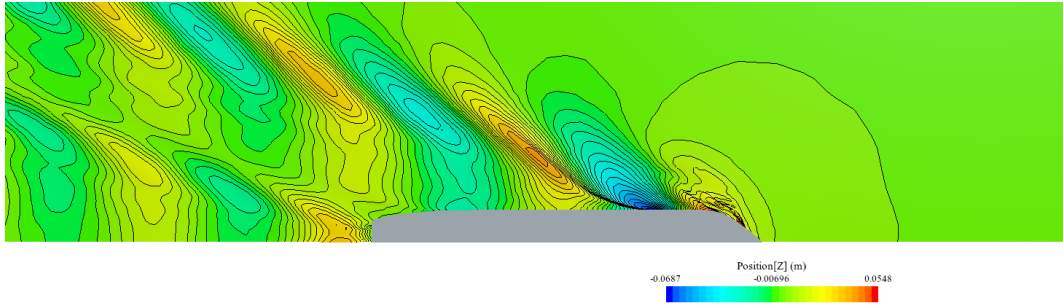
$V_s = 15kn$



$$V_s = 16kn$$



$$V_s = 17kn$$



$$V_s = 18kn$$

3. MODEL TEST AND RANS SOLVER UNCERTAINTY ANALYSIS

2.1 MODEL TEST

To assess the uncertainty and computational accuracy of the RANS solver, resistance tests were conducted in the towing tank at Wuhan University of Technology. The towing tank is a member facility of the International Towing Tank Conference (I.T.T.C.). It has a total length of 132 meters, a width of 10.4 meters, and a depth of 2.0 meters. The towing carriage operates at speeds ranging from 0.06 m/s to 7.00 m/s, controlled by a computer-based closed-loop system. The speed accuracy is within ± 1.0 mm/s for speeds between 0.06 m/s and 1.0 m/s, and within $\pm 0.1\%$ for speeds between 1.0 m/s and 7.0 m/s.

All experimental data were automatically collected by a data acquisition system. The model resistance was measured using an R63 strain gauge-type dynamometer with an accuracy of 0.1%.

Prior to each test, the measurement system was calibrated and validated. The still water interval between two consecutive towing tests was approximately 13 minutes.

The ship model was constructed from wood and coated with yellow paint, as shown in Fig. 6. The model maintains geometric similarity with the full-scale vessel and features a smooth surface finish. The manufacturing accuracy of the model met the following tolerances: less than 0.05% in the longitudinal direction, less than 0.1% in the transverse direction, and less than 1 mm deviation between each station and the corresponding construction template. After fabrication, a metal trip wire was installed at Station 19 of the model to minimize errors caused by viscous effects.。

The scale and principal particulars of the ship model used in the experiment are listed in Table 1.

Table. S1. Principal Particulars of the Designer Scheme ship Model and the Full-Scale Ship

Parameter	Symbol	Unit	Full-Scale	Model
Beam	B	m	17.60	0.5867
Draft	T	m	5.20	0.1733
Length at Waterline	Lwl	m	106.00	3.5333
Displacement Volume	V	m ³	7207.7	0.2670
Block Coefficient	Cb	-	0.743	0.743
Scale Ratio	λ	-	30	



Fig. S6 Model test of Designer Scheme ship in 1.3149m/s condition.

The model test result as shown in Table 2.

Table 2. The model test result of the Designer Scheme ship

V_s (kn)	Fr -	V_m (m/s)	R_m (N)
5.00	0.0798	0.4696	1.3393
6.00	0.0958	0.5635	1.8816
7.00	0.1117	0.6575	2.4931
8.00	0.1277	0.7514	3.2437
9.00	0.1437	0.8453	4.0394
10.00	0.1596	0.9392	5.0155
11.00	0.1756	1.0332	6.2455

12.00	0.1915	1.1271	7.2627
13.00	0.2075	1.2210	9.0973
14.00	0.2235	1.3149	10.9868
15.00	0.2394	1.4089	13.6681
16.00	0.2554	1.5028	16.7188
17.00	0.2713	1.5967	21.1582
18.00	0.2873	1.6906	29.8498

2.2 RANS SOLVER

The RANS simulations in this study were conducted using the commercial CFD software STAR-CCM+, employing an implicit unsteady solver. The computational domain setup is illustrated in Fig. 7, and an overview of the mesh configuration is shown in Fig. 8.

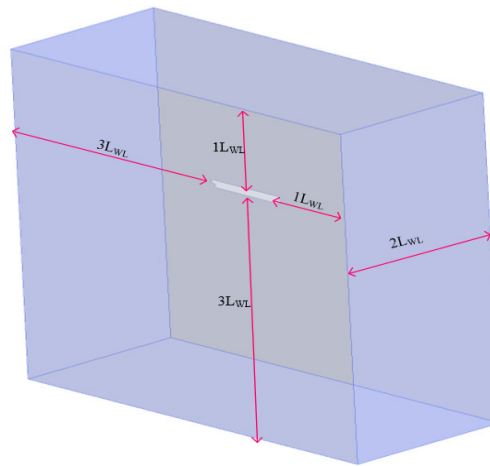


Fig.S7 The computational domain setup.

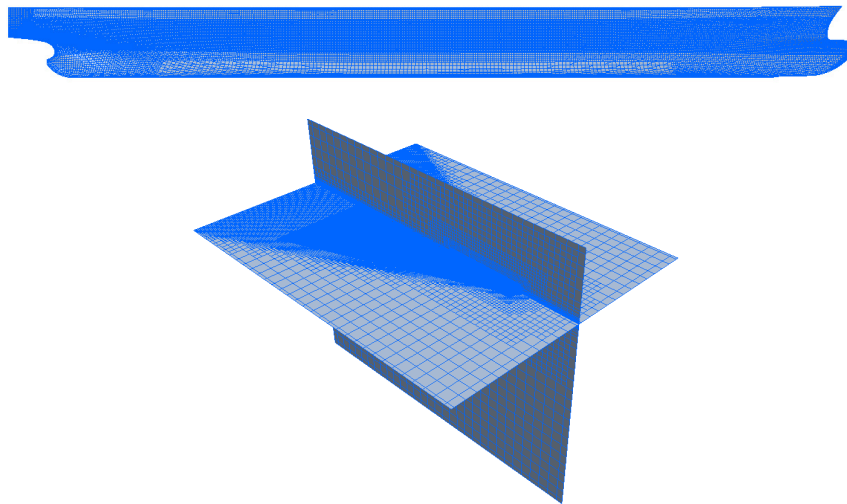


Fig. S8. Mesh layout.

The computational mesh was generated using the Trimmed Cell Mesher utility, producing a baseline mesh of approximately 2.1 million cells for half of the hull geometry. The mesh was refined in regions near the hull and along the expected Kelvin wake angle, where hull-generated waves propagate.

To maintain a reasonable total cell count while resolving near-wall flows, a wall-function approach was adopted. Accordingly, a prism layer mesh was incorporated to ensure proper resolution of the boundary layer.

The simulations were performed using the Local Time Stepping (LTS) technique to efficiently compute steady-state solutions. The Volume of Fluid (VoF) method was applied to capture the interface dynamics in the multi-phase flow environment (air and water).

Given the turbulent nature of the flow around the ship, the Shear Stress Transport (SST) $k-\omega$ model was employed for turbulence closure, which offers a good balance between near-wall accuracy and robustness in free-stream regions.

To verify the accuracy of the CFD model, a preliminary validation was performed by comparing the predicted calm water resistance of the model-scale Designer Scheme hull against the corresponding experimental fluid dynamics (EFD) results.

The grid uncertainty analysis was performed in accordance with the procedures recommended by the International Towing Tank Conference (ITTC) for CFD uncertainty evaluation. A grid refinement ratio of $r = 1.1$ was selected in a single direction to generate three levels of meshes: a coarse mesh, the baseline mesh (as described above), and a fine mesh.

The uncertainty analysis followed a two-step process:

Grid Convergence Assessment:

The convergence behavior of the simulation results across the three mesh levels was evaluated using Equations (1)–(3), based on ITTC guidelines. This step determines whether the solution is monotonically convergent, oscillatory, or divergent.

$$\varepsilon_{12} = S_1 - S_2 \quad (1)$$

$$\varepsilon_{23} = S_2 - S_3 \quad (1)$$

$$R_G = \varepsilon_{12}/\varepsilon_{23} \quad (1)$$

where ε_{12} represents the difference between the fine and medium grid solutions, ε_{23} represents the difference between the medium and coarse grid solutions. R_G is the grid convergence ratio.

Based on the value of the grid convergence ratio R_G , the convergence behavior of the computed results can be classified into four categories:

Oscillatory Divergence: if $R_G < -1$, the solution exhibits oscillatory divergence.

Oscillatory Convergence: if $-1 < R_G < 0$, the solution is oscillatory but converging

Monotonic Convergence: if $0 < R_G < 1$, the solution is monotonically converging.

Monotonic Divergence: if $R_G > 1$, the solution exhibits monotonic divergence.

Grid Uncertainty Estimation:

Following the convergence analysis, the Generalized Richardson Extrapolation method was employed to estimate the grid uncertainty component U_G , using Equations (4)-(8). This approach quantifies the numerical uncertainty associated with the spatial discretization error.

$$P = |\ln(\varepsilon_{23}/\varepsilon_{12})/\ln r| \quad (4)$$

$$\delta = \varepsilon_{12}/(r^P - 1) \quad (5)$$

$$C_G = (r^P - 1)/(r^{P_{th}} - 1) \quad (6)$$

$$\delta^* = C_G \delta \quad (7)$$

$$U_G = [|1 - C_G|]|\delta| \quad (8)$$

where p denotes the order of accuracy of the numerical scheme. δ represents the discretization error, while δ^* is the estimated discretization error. C_G is the correction factor used in the generalized Richardson extrapolation. p_{th} refers to the theoretical order of accuracy of the numerical scheme in the asymptotic range, i.e., when the grid spacing tends to zero and the solution approaches the asymptotic regime. In practice, p_{th} is typically taken as 2 for second-order accurate scheme.

The final total uncertainty is calculated using Equation (9), where $U_D=2\%EFDresult$.

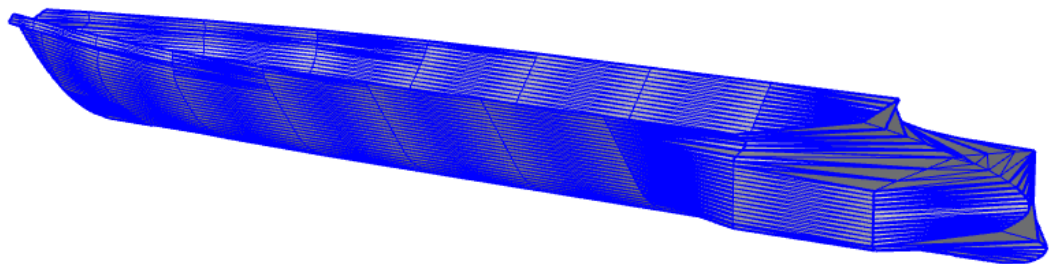
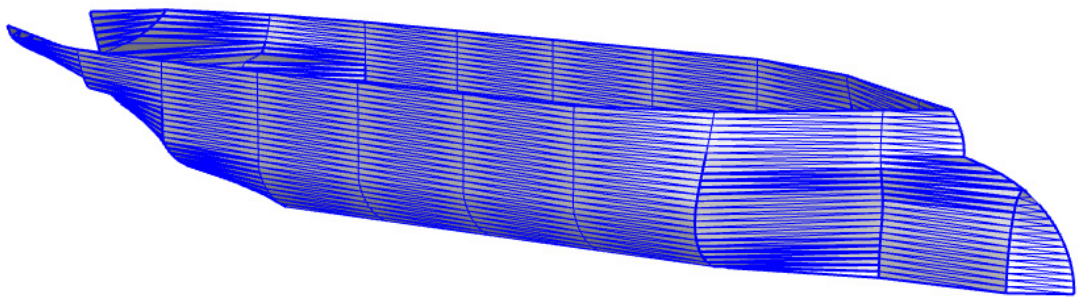
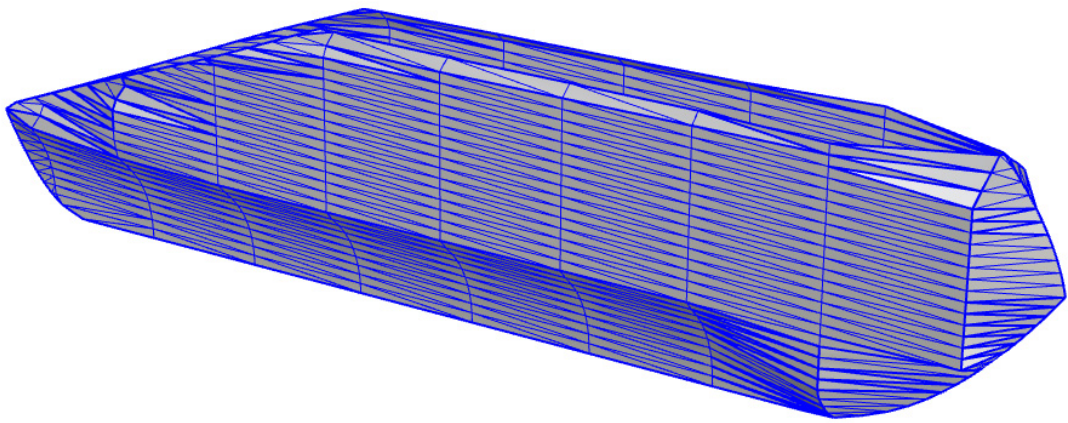
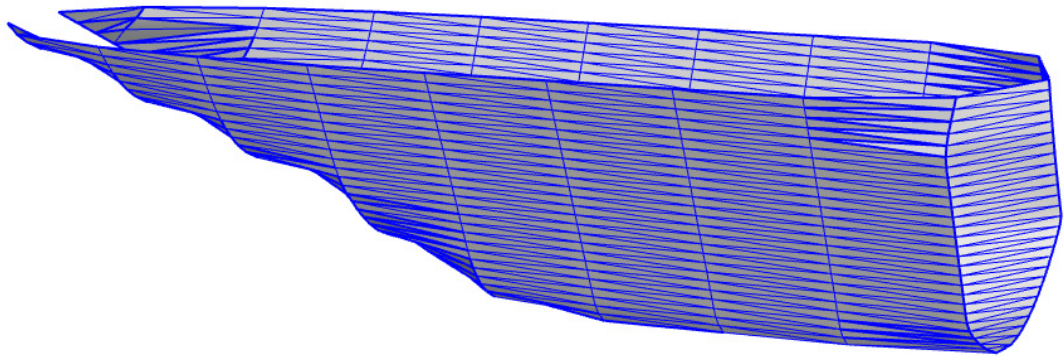
$$U_V^2 = U_D^2 + U_G^2 \quad (9)$$

The uncertainty analysis results of the RANS solver at different ship speeds are summarized in Table 3.

V_s	Fr	V_m	EFD_Rm	CFD_fine_Rm	$CFD_baseline_Rm$	CFD_coarse_Rm	RG	$Error_fine$	$Error_baseline$	$Error_coarse$	UD	U_v
(kn)		(m/s)	N	N	N	N		$\%EFD_Rm$	$\%EFD_Rm$	$\%EFD_Rm$	$\%EFD_Rm$	$\%EFD_Rm$
5.0000	0.0798	0.4696	1.3393	1.3395	1.3374	1.3253	0.1798	0.019%	0.143%	1.040%	0.0200	2.13%
6.0000	0.0958	0.5635	1.8816	1.8668	1.8634	1.8452	0.1864	0.784%	0.965%	1.932%	0.0200	2.16%
7.0000	0.1117	0.6575	2.4931	2.4964	2.4856	2.4615	0.4486	0.132%	0.302%	1.267%	0.0200	2.63%
8.0000	0.1277	0.7514	3.2437	3.2314	3.2233	3.1903	0.2472	0.380%	0.631%	1.648%	0.0200	2.29%
9.0000	0.1437	0.8453	4.0394	4.0171	4.0021	3.9659	0.4144	0.553%	0.924%	1.820%	0.0200	2.50%
10.0000	0.1596	0.9392	5.0155	4.9947	4.9694	4.9358	0.7530	0.416%	0.920%	1.590%	0.0200	2.18%
11.0000	0.1756	1.0332	6.2455	6.1998	6.1845	6.1683	0.9470	0.732%	0.977%	1.236%	0.0200	3.78%
12.0000	0.1915	1.1271	7.2627	7.2546	7.2501	7.1558	0.0482	0.112%	0.174%	1.472%	0.0200	2.02%
13.0000	0.2075	1.2210	9.0973	9.0175	8.9775	8.9122	0.6125	0.877%	1.317%	2.035%	0.0200	2.44%
14.0000	0.2235	1.3149	10.9868	10.8588	10.8287	10.7483	0.3748	1.165%	1.439%	2.171%	0.0200	2.30%
15.0000	0.2394	1.4089	13.6681	13.6050	13.5384	13.3688	0.3925	0.462%	0.949%	2.190%	0.0200	2.83%
16.0000	0.2554	1.5028	16.7188	16.6550	16.5461	16.3439	0.5385	0.382%	1.033%	2.243%	0.0200	3.08%
17.0000	0.2713	1.5967	21.1582	21.1176	21.0095	20.7599	0.4331	0.192%	0.703%	1.883%	0.0200	2.86%
18.0000	0.2873	1.6906	29.8498	29.9268	29.7946	29.4559	0.3905	0.258%	0.185%	1.320%	0.0200	2.71%

s shown in the table, all simulation uncertainties are smaller than U_v . Therefore, we consider the RANS solver to be reliable.

4. OTHER MATERIALS



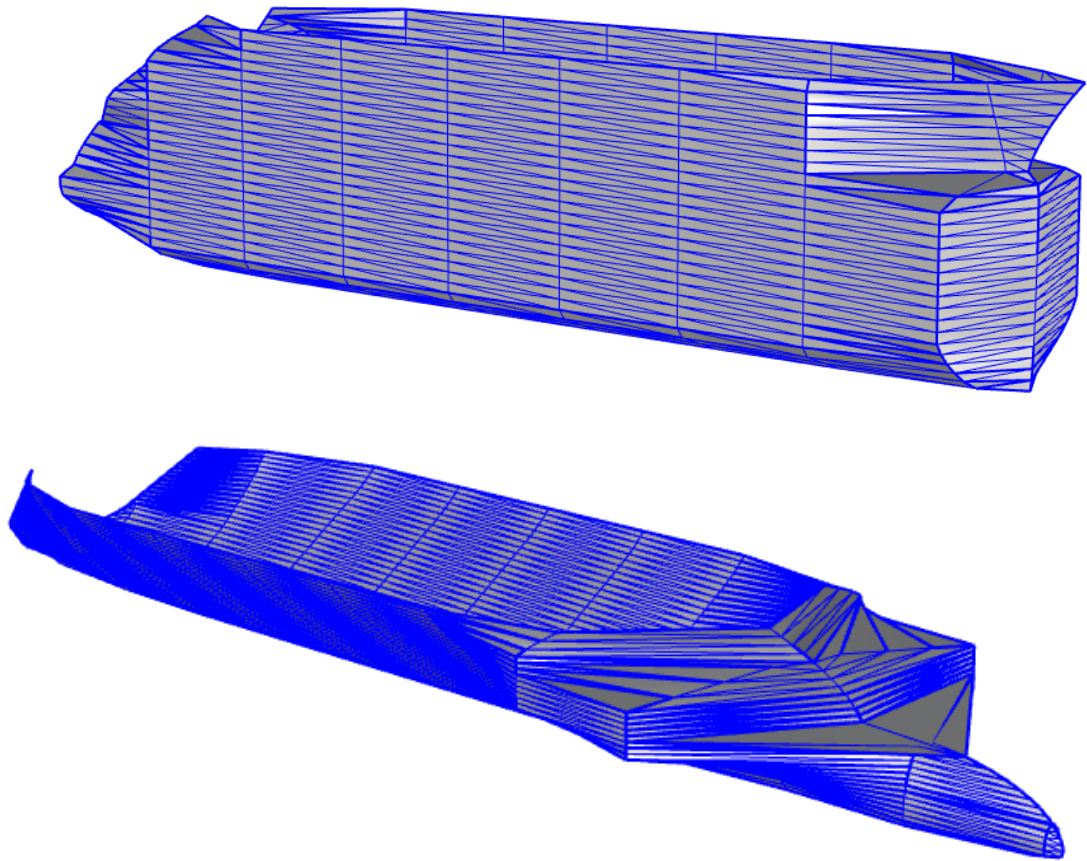


Fig.S9 The ship geometries in the dataset looks like uncommon geometries.